Polymer Journal, Vol. 37, No. 4, pp. 324–331 (2005)

Small-Angle X-Ray Scattering from Polystyrene Polymacromonomers in Cyclohexane

Keiji AMITANI, Ken TERAO, Yo NAKAMURA,[†,††] and Takashi NORISUYE

Department of Macromolecular Science, Osaka University, 1-1 Machikaneyama-cho, Toyonaka 560-0043, Japan

(Received December 10, 2004; Accepted January 6, 2005; Published April 15, 2005)

ABSTRACT: Small-angle X-ray scattering measurements have been made on seven polymacromonomer samples consisting of polystyrene with a fixed side chain length of 15 styrene residues in cyclohexane at 34.5 °C to obtain the z-average mean-square radius of gyration $\langle S^2 \rangle_z$ and the particle scattering function $P(\theta)$. The dependence of $\langle S^2 \rangle_z$ on the weight-average molecular weight M_w, which ranges from 5.1×10^3 to 1.8×10^5, is described by the wormlike chain with the model parameters explaining previous light scattering $\langle S^2 \rangle_z$ data for high molecular weights (6×10^5–7×10^6), when the effect of the chain diameter d and that of side chains near the main-chain ends on the polymacromonomer contour length L are incorporated into analysis. Scattering profiles in the form of the Kratky plot are also explained by the recent theory for the wormlike chain with a circular cross section unless the axial ratio L/d is less than 2, *i.e.*, unless M_w is lower than 2.6×10^4. The conventional cross-section plot, *i.e.*, the plot of $\ln[kP(\theta)]$ *vs.* k^2 with slope $-d^2/16$, is found to be applicable to samples with $L/d > 2$, where k denotes the magnitude of the scattering vector. It is concluded from further analysis of the $\langle S^2 \rangle_z$ data combined with previous transport coefficient data that the wormlike cylinder model, a smeared model for regular comb polymers, consistently explains the molecular weight dependence of $\langle S^2 \rangle_z$, intrinsic viscosity, and translational diffusion coefficient for the polystyrene polymacromonomer in cyclohexane over a broad range of molecular weight. The applicability of a semiflexible comb model consisting of wormlike main and side chains to $\langle S^2 \rangle_z$ and $P(\theta)$ is also examined. [DOI 10.1295/polymj.37.324]

KEY WORDS Small-Angle X-Ray Scattering / Polymacromonomer / Comb Polymer / Radius of Gyration / Scattering Function / Theta Solvent / Chain Thickness / End Effect /

Recent experimental studies on polymer solutions revealed that brush-like polymers behave as stiff chains in dilute solution though they are composed only of flexible chains.[1–6] In hope of obtaining further structural information, especially on the main-chain stiffness, we investigated polymacromonomers consisting of polystyrene in cyclohexane at 34.5 °C (a theta solvent) and in toluene at 15 °C (a good solvent) by static[7–9] and dynamic light scattering[10] and viscometry.[9,11] The molecular weight dependence of the z-average mean-square radius of gyration $\langle S^2 \rangle_z$ (> 100 nm^2) for a few series of samples with fixed side chain lengths was found to be explained by the contour of the wormlike chain with[12] or without[13] excluded volume, so that no structural information on the polymer thickness (and hence on the side chains) was obtained from light-scattering $\langle S^2 \rangle_z$. On the other hand, analyses of intrinsic viscosities $[\eta]$ and translational diffusion coefficients D gave values of the chain diameter d in addition to the wormlike chain parameters determining the contour, though end effects arising from side chains near the main-chain ends had to be considered.[9–11] The estimated d for each polymer happened to be comparable to what is expected from the molar mass of the side chain.

The theories[14–16] for $[\eta]$ and D of the wormlike chain used for the aforementioned analyses should be accurate for stiff chains, but they may involve a few problems concerning d. Firstly, though not all, unreasonable values of d were estimated for a few typical stiff polymers on the basis of these theories or equivalents.[17] Secondly, the chain length dependence of $[\eta]$ or D for stiff but thick wormlike chains is rather similar to that for flexible chains[10,11] for which those theories are less accurate. Thirdly, no theoretical $[\eta]$ for short, thick cylinders with flexibility is available, so that the theory[16] based on the touched-bead model (instead of the cylinder model) was used in our estimation of d.[9,11]

In view of these theoretical problems, we deemed it necessary to investigate by small-angle X-ray scattering[18] (SAXS) the particle scattering function $P(\theta)$ and the radius of gyration for polymacromonomer samples of low molecular weight, for which the effect of d should be significant. The present study was thus undertaken to see whether data of $\langle S^2 \rangle_z$ and $P(\theta)$ for a series of polymacromonomer samples (F15) with a fixed side chain length of 15 styrene residues in cyclohexane at 34.5 °C are consistent with the structural information from $[\eta]$ and D. Wataoka *et al.*[19] already

[†]To whom correspondence should be addressed (E-mail: yonaka@molsci.polym.kyoto-u.ac.jp).
[††]Present Address: Department of Polymer Chemistry, Kyoto University, Katsura, Kyoto 615-8510, Japan.

attempted to estimate d of polymacromonomers by SAXS, but they used the expressions for $P(\theta)$ of ellipsoids and elliptic cylinders probably because no relevant theory for cylindrical wormlike chains was available. Quite recently, Nakamura and Norisuye[20] calculated $P(\theta)$ for a wormlike chain with a circular cross section according to the procedure of Nagasaka *et al.*[21] We therefore analyze the present $P(\theta)$ data using this new theory. We also analyze the $\langle S^2\rangle_z$ and $P(\theta)$ data in terms of a comb model that explicitly considers the side chains in a polymacromonomer molecule.

EXPERIMENTAL

Samples and Preparation of Solutions

Seven polymacromonomer samples consisting of polystyrene were chosen from a series (F15) of previously investigated samples,[8,10,11] which had been synthesized from the same macromonomer having the benzyl group at one end of each molecule. The weight-average molecular weight M_w and the ratio of M_w to the number-average molecular weight M_n of this macromonomer were 1650 and 1.09, respectively. Molecular weights from light scattering and M_w/M_n values from gel permeation chromatography for the polymacromonomer samples[8] studied are shown in the second and third columns of Table I.

Each test sample was dried *in vacuo* for more than 12 h just before use. Its solutions were prepared by mixing the weighed amount of the polymer with cyclohexane, which was fractionally distilled after being refluxed over sodium for 5 h. The polymer mass concentration c was calculated from the polymer weight fraction and the solution density.

Small-Angle X-Ray Scattering

Intensities of X-ray scattered from polymacromonomer F15 in cyclohexane at 34.5 °C were measured on the point-focusing system developed previously.[22] This system is briefly described below.

X-Ray is generated from the copper rotating anode of a Rigaku RU-200 X-ray generator operated at 30 kV and 150 mA and is focused by two elliptic mirrors joined in the side-by-side manner. The mirror is made of 50 alternate layers of tungsten and boron carbide, whose spacing changes gradually from one end to the other according to the reflection angle of the K_α line (wavelength $\lambda_0 = 0.154$ nm). The focused X-ray beam passes through two pinhole slits to remove the K_β component and X-ray caused by parasitic scattering at the mirror surface. The test solution in a quartz-glass capillary (1.5 mm in diameter) is kept within ±0.1 °C by circulation of temperature-regulated water through a capillary holder. The scattered X-ray is detected on an imaging plate (IP) as a two-dimensional image, which is processed with an IP reading system (Rigaku R-AXIS DS).[23] The distance from the capillary to the detector is 565 mm. The desired intensities $I(\theta)$ are obtained as a function of scattering angle θ by integration of intensities over a narrow angular range from $\theta - \Delta\theta$ and $\theta + \Delta\theta$ with $\Delta\theta = 0.005°$–$0.025°$. We note that no significant error is introduced even for $\Delta\theta = 0.04°$ if $\langle S^2\rangle_z$ is less than 100 nm^2.[23]

Four to five solutions with different concentrations were measured for each sample; c was in the range between 1.1×10^{-2} and 4.0×10^{-2} g cm^{-3} for the highest molecular weight sample F15-9 and between 1.0×10^{-1} and 3.2×10^{-1} g cm^{-3} for the lowest molecular weight sample F15-15. Intensity data were accumulated for 6 h for each solution. The solvent intensity was measured before and after the measurement of every solution and its mean was subtracted from $I(\theta)$ for the solution to obtain the excess scattering intensity $\Delta I(\theta)$. The resulting $c/\Delta I(\theta)$ values at fixed θ ($< 2.0°$) were insensitive to c, as expected for the theta solvent.[8] They were extrapolated to infinite dilution using the square-root plot of $[c/\Delta I(\theta)]^{1/2}$ *vs.* c; those for $\theta > 2.0°$ were discarded because $\Delta I(\theta)$ values at such high angles were inaccurate. We note that no correction for X-ray absorption by the solution is necessary at infinite dilution.

Table I. Molecular weights[8] and results from SAXS measurements on polystyrene polymacromonomer (F15) samples in cyclohexane at 34.5 °C

Sample	$M_w/10^5$	M_w/M_n	$\langle S^2\rangle_z$/nm^2	d/nm
F15-9	1.75	1.10	34	5.1
F15-10	1.23	1.10	23	5.0
F15-11	0.614	1.08	10.5	4.7
F15-12	0.474	1.09	9.2	4.7
F15-13	0.260	1.09	5.4	4.5
F15-14	0.108		4.2	4.7
F15-15	0.0514		3.5	4.7

RESULTS

Figure 1 shows the angular dependence of $[c/\Delta I(\theta)]^{1/2}_{c=0}$, the infinite-dilution value of $[c/\Delta I(\theta)]^{1/2}$, for samples F15-9 and F15-10 and that of $\ln[\Delta I(\theta)/c]_{c=0}$ for the rest, both in a low-angle region; we expected the Guinier plot of $\ln[\Delta I(\theta)/c]_{c=0}$ *vs.* k^2 to be linear up to a larger k than the square-root plot for low molecular weight samples. Here, k is the magnitude of the scattering vector **k**. The z-average mean-square radii of gyration evaluated from the indicated straight lines are summarized in the fourth column of Table I.

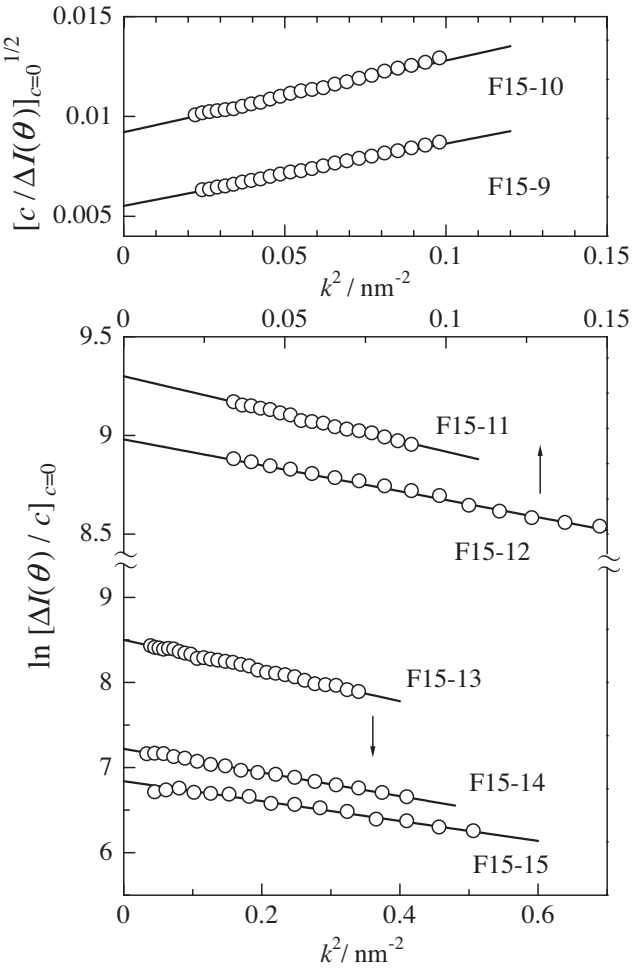

Figure 1. Plots of $[c/\Delta I(\theta)]_{c=0}^{1/2}$ and $\ln[\Delta I(\theta)/c]_{c=0}$ against k^2 for the indicated samples of polymacromonomer F15 in cyclohexane at 34.5 °C.

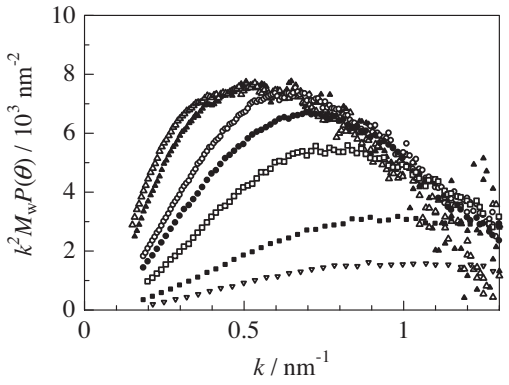

Figure 2. Reduced Kratky plots for samples of polystyrene polymacromonomer F15 in cyclohexane at 34.5 °C: △, F15-9; ▲, F15-10; ○, F15-11 (reproduction from ref 22); ●, F15-12; □, F15-13; ■, F15-14; ▽, F15-15.

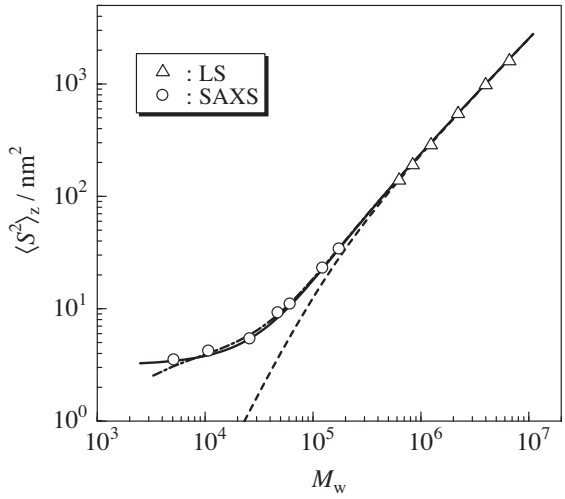

Figure 3. Molecular weight dependence of $\langle S^2\rangle_z$ determined by SAXS (circles) and light scattering (triangles) measurements for polystyrene polymacromonomer F15 in cyclohexane at 34.5 °C. The solid and dashed lines show theoretical values for the wormlike chain with and without the effects from thickness and chain ends. The dot-dashed line represents theoretical values for comb polymers composed of wormlike subchains (eqs A-1–A-3).

Figure 2 shows the scattering functions in the form of the reduced Kratky plot of $M_w k^2 P(\theta)$ against k for all the samples studied. We have evaluated $P(\theta)$ from $[c/\Delta I(0)]_{c=0}/[c/\Delta I(\theta)]_{c=0}$, where $[c/\Delta I(0)]_{c=0}$ denotes the value of $[c/\Delta I(\theta)]_{c=0}$ at $\theta = 0$. As is expected for thick polymer chains with small axial ratios, each curve has a broad peak. The peak top moves to a larger k and its height decreases with decreasing molecular weight. Except for the two samples with low degrees of polymerization, the scattering curves for different samples almost merge at large k.

DISCUSSION

Radius of Gyration

The mean-square radius of gyration $\langle S^2\rangle_{KP}$ of the Kratky–Porod (KP) chain[24] is expressed by[13]

$$\langle S^2\rangle_{KP} = \frac{L}{6\lambda} - \frac{1}{4\lambda^2} + \frac{1}{4\lambda^3 L} - \frac{1}{8\lambda^4 L^2}[1 - \exp(-2\lambda L)] \qquad (1)$$

where λ^{-1} and L are the Kuhn segment length and the contour length of the chain, respectively. The latter is related to the molecular weight M by

$$L = M/M_L \qquad (2)$$

with M_L being the molar mass per unit contour length of the chain.

The data of $\langle S^2\rangle_z$ from the present SAXS and previous light scattering[8] measurements for the F15 polymacromonomer in cyclohexane at 34.5 °C are plotted double-logarithmically against M_w in Figure 3. The dashed line represents the values calculated from eqs 1 and 2 with $M_L = 6200\,\text{nm}^{-1}$ and $\lambda^{-1} = 9.5$

nm, which were determined by Terao *et al.*[8] so as to give the closest fit to the triangles. This line deviates remarkably downward from the circles for M_w below 10^5, suggesting a significant effect of chain thickness on $\langle S^2\rangle_z$. When this effect was taken into account according to the equation[25]

$$\langle S^2\rangle = \langle S^2\rangle_{KP} + (d^2/8) \tag{3}$$

for the KP chain with a uniform diameter d using $d = 4.7$ nm (determined[11] from $[\eta]$), the calculated curve rose but was still appreciably below the circles (not shown). Although the choice of a larger d improved the agreement to some extent, no quantitative agreement was reached by adjustment of d. This was also the case in the analyses of $[\eta]$ and D.[9–11]

In our previous work, Terao *et al.*[10,11] demonstrated significant end effects on $[\eta]$ and D at relatively low molecular weights by introducing a parameter δ defined by

$$L = M/M_L + \delta \tag{4}$$

where δ stands for the apparent contribution of side chains near the main-chain ends to L (see Figure 3 of ref 11). Terao *et al.* found that a δ value of 2.2 nm (with $M_L = 6300\,\text{nm}^{-1}$, $\lambda^{-1} = 9.5$ nm, and $d = 4.7$ nm) explains the M_w-dependence of $[\eta]$ for the F15 polymacromonomer in cyclohexane (down to $M_w \sim 2 \times 10^4$).[11] They assigned a slightly larger δ of 2.5 (± 0.3) nm to obtain a good agreement between theory and experiment for D;[10] although the other parameters from D and $[\eta]$ also slightly differed, the discrepancy was hardly beyond their uncertainty. The solid curve in Figure 3 calculated with $\delta = 2.2$ nm for the above parameter set ($M_L = 6200\,\text{nm}^{-1}$, $\lambda^{-1} = 9.5$ nm, and $d = 4.7$ nm) is seen to fit all the data points very closely. Hence, we may conclude that the wormlike chain model with the thickness and end effects is capable of consistently explaining our $\langle S^2\rangle_z$, $[\eta]$, and D data for the polymacromonomer in the theta state. We wish to point out that the $\langle S^2\rangle_z$ data in the figure do not allow separate estimation of d and δ and are equally fitted by theoretical curves for pairs of parameters in the range $3.8 < d/\text{nm} < 5.0$ and $2.1 < \delta/\text{nm} < 4.2$.

It is interesting to see whether a semiflexible comb model chain explicitly taking into account side chains is applicable to our $\langle S^2\rangle_z$ data. We here consider a simple model in which each side chain is a wormlike coil with contour length L_s and Kuhn length λ_s^{-1} and linked to the main chain of contour length L and Kuhn length λ^{-1} by a universal joint. The expression for $\langle S^2\rangle$ of this comb, derived by Nakamura *et al.*,[26] is given by eq A-1 with eqs A-2 and A-3 in the Appendix as a function of L_s, λ_s^{-1}, L, λ^{-1}, and p (the number of side chains in the molecule). For the F15 polymacromonomer, we obtain $L_s = 3.92$ nm from the molecular weight of the side chain divided by the linear mass density of linear polystyrene ($390\,\text{nm}^{-1}$)[27] in cyclohexane at 34.5 °C.

The dot-dashed curve in Figure 3, calculated from eqs A-1–A-3 with $M_L = 6200\,\text{nm}^{-1}$, $\lambda^{-1} = 9.5$ nm, $L_s = 3.92$ nm, and $\lambda_s^{-1} = 6$ nm, closely fits the data points. The last parameter, chosen to fit the data, is much larger than that known for linear polystyrene (2 nm)[27] in the same solvent though it may be somewhat overestimated owing to the universal joint invoked for the junction of the main and side chains in the model. If literally taken, this larger λ_s^{-1} implies that the side chains of the polymacromonomer are more extended than an isolated polystyrene chain. The average diameter of the polymacromonomer molecule is calculated to be 5.8 nm if it is equated to the root-mean-square end-to-end distance for the contour length $2L_s$. This diameter does not differ much from the values 4.7–5.1 nm estimated from $[\eta]$ and D on the basis of the smeared cylinder model.

Scattering Functions

Use is often made of the cross-section plot of $\ln[kP(\theta)]$ *vs.* k^2 to determine d of a polymer chain from scattering data.[18] Figure 4 shows this type of plot for five high molecular weight samples (data for F15-11 are the reproduction from ref 22). Except for a very low k^2 region, the experimental data for each sample can be fitted by a straight line (dashed line) over a wide range of k^2, as was found by Wataoka *et al.*[19] for polymacromonomers consisting of the poly(methyl methacrylate) or polystyrene backbone and polystyrene side chains in toluene at non-zero concentrations. This linearity is consistent with our recent calculation[20] that theoretical $\ln[kP(\theta)]$ for the wormlike chain with a finite thickness is approximately linear with a slope fairly close to $-d^2/16$ (the conventionally assumed slope) in a wide range of k^2. Equating the slope of each straight line to $-d^2/16$, we obtain $d = 5.1$, 5.0, 4.7, 4.7, and 4.0 nm for F15-9, F15-10, F15-11, F15-12, and F15-13, respectively. Except for F15-13, these d values are essentially constant.

In Figures 5a and 5b, the Kratky plots for all the samples are compared with theoretical solid curves computed from Nakamura and Norisuye's theory[20] for the wormlike cylinder with $M_L = 6200\,\text{nm}^{-1}$, $\lambda^{-1} = 9.5$ nm, $\delta = 2.2$ nm and an appropriately chosen d for each sample. Except for the two lowest molecular weight samples, the agreement between theory and experiment is satisfactory. The chosen d values, presented in the fifth column of Table I, are essentially invariable, being 4.8 ± 0.3 nm, and those for samples F15-9 through F15-12 agree with what was esti-

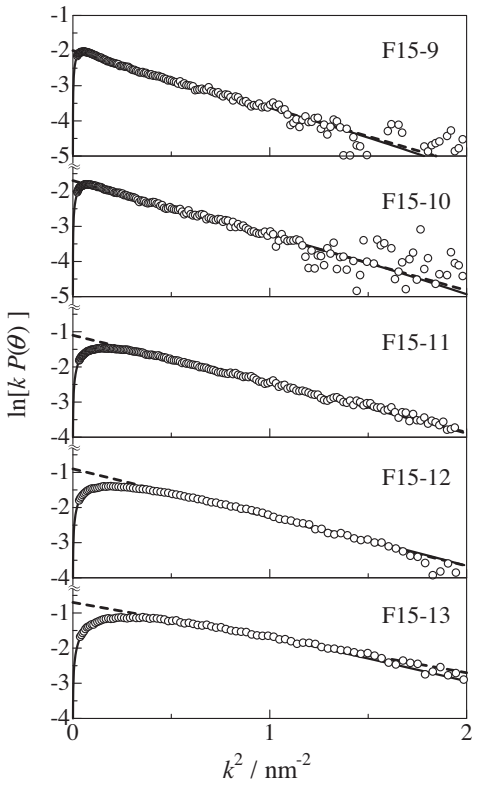

Figure 4. Cross-section plots for five high molecular weight samples in cyclohexane at 34.5 °C. Dashed lines, empirical linear fits; solid lines, calculated values for the wormlike cylinder model[20] (see the text).

mated from the cross-section plot in Figure 4. The solid lines in this figure actually represent Nakamura and Norisuye's theoretical values for the parameter sets used in Figures 5a and 5b, so that their overlaps with the dashed lines at not-too small k^2 for these samples are consistent with this agreement in d. For sample F15-13, however, the two lines in Figure 4 do not overlap for $k^2 > 1\,\mathrm{nm}^{-2}$, yielding different d values. Hence, the conventional slope $-d^2/16$ of the cross-section plot cannot be used for this low molecular weight sample whose axial ratio (L/d) is only about 1.4. In any event, the present $P(\theta)$ data for samples F15-9 through F15-13 are also explained by essentially the same parameters describing $[\eta]$ and D for the polystyrene polymacromonomer in cyclohexane.

In Figure 5b, the solid curves for F15-14 and F15-15 do not fit the scattering intensity data at k larger than $1\,\mathrm{nm}^{-1}$. Since the number of side chains is small (less than 7) for these low molecular weight samples, the cylindrical model should be crude at such high scattering angles where X-ray sees the relatively local structure of the molecules. In this situation, it is worthwhile to examine $P(\theta)$ for the semiflexible comb model mentioned in relation to the M_w-dependence of $\langle S^2\rangle_z$.

The dot-dashed lines in Figure 5b show the $k^2P(\theta)$

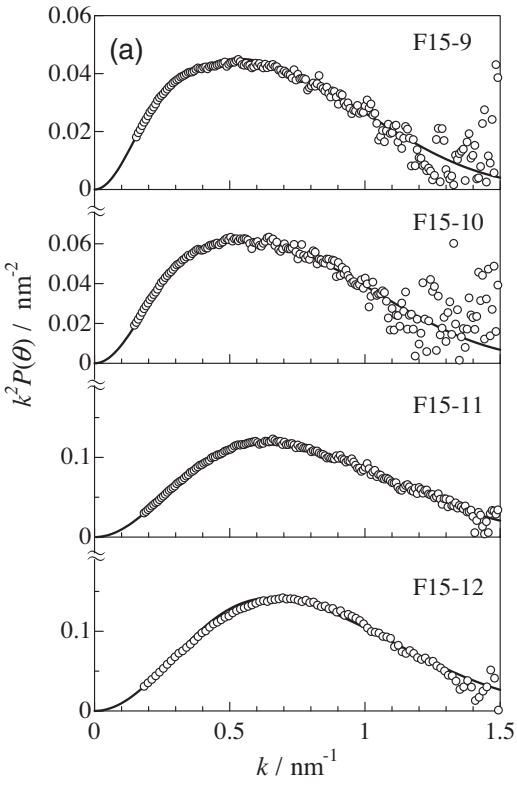

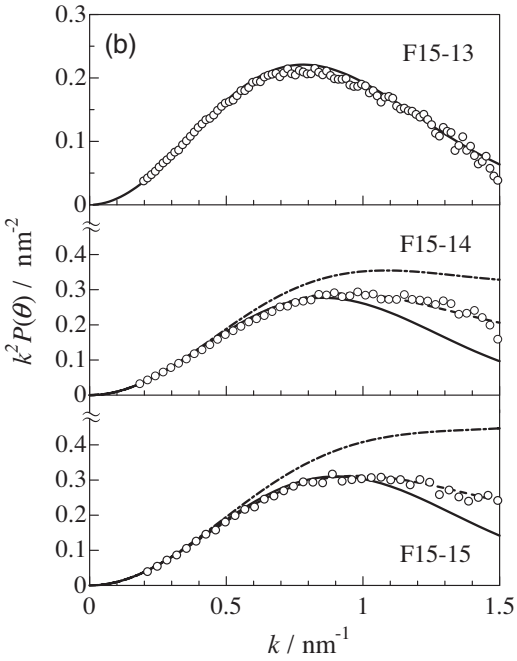

Figure 5. Kratky plots for samples F15-9, F15-10, F15-11, and F15-12 (a) and for F15-13, F15-14, and F15-15 (b) in cyclohexane at 34.5 °C. Solid lines, theoretical values for the wormlike cylinder model[20] (see the text); dot-dashed lines, values for the semiflexible comb model (eqs A-4–A-9); dashed lines, values for the semiflexible touched-bead comb model (eq A-10 with eqs A-4–A-9).

values calculated for this comb model from eqs A-4 through A-9 in the Appendix with the same parameter set as that for $\langle S^2\rangle$ of the comb in Figure 3. These

curves deviate considerably upward from the data points for the respective samples, and their deviations are even larger than those observed for the cylinder model. If the thickness of the main and side chains is taken into account on the basis of the touched-bead model (eq A-10 in the Appendix) with the bead diameter d_b taken as 2.0 nm for F15-14 and 2.3 nm for F15-15, the scattering curves for the samples come very close to the data points, as indicated by the dashed lines in the figure (d_b should not be confused with the polymacromonomer diameter d). This substantiates the importance of the chain thickness to $P(\theta)$ for the polymacromonomer samples at high scattering angles, but the good agreement must be accepted with some reservation because the chosen diameters are appreciably larger than what is expected from the chemical structure of the styrene residue (about 1 nm). Applying the comb model to F15 samples of higher molecular weight with d_b as an adjustable parameter, we obtain similar or even larger diameters. Thus the present comb model explains $P(\theta)$ of the F15 polymacromonomer in cyclohexane at the theta point only for $k < 1\,\mathrm{nm}^{-1}$, and the behavior at higher scattering angles remains to be seen theoretically on a more elaborate model. It should be noted that d_b hardly affects $\langle S^2\rangle$ and hence $P(\theta)$ at small k even for the lowest molecular weight sample studied.

Hydrodynamic Factors

Combining the present $\langle S^2\rangle_z$ and previous $[\eta]$ and D data, we obtain the hydrodynamic factors Φ and ρ defined by $[\eta]M_w/(6\langle S^2\rangle_z)^{3/2}$ and $6\pi\eta_0 D\langle S^2\rangle_z^{1/2}/kT$, respectively, with η_0 being the solvent viscosity. Figure 6 shows that Φ changes with molecular weight and has a pronounced maximum around $M_w = 3 \times 10^4$ whereas ρ^{-1} stays almost constant.

The solid line for ρ^{-1} in the figure calculated from the theory of Yamakawa and Fujii[14] ($M_w \geq 1.2 \times 10^5$) or Norisuye *et al.*[15] ($M_w \leq 1.2 \times 10^5$) for the translational friction coefficient of a wormlike cylinder and from eqs 1–4 with $M_L = 6200\,\mathrm{nm}^{-1}$, $\lambda^{-1} = 9.5\,\mathrm{nm}$, $d = 4.7\,\mathrm{nm}$, and $\delta = 2.2\,\mathrm{nm}$ comes close to the data points. This is expected because both D and $\langle S^2\rangle_z$ can separately be explained by the wormlike chain model; the slightly but systematically larger experimental ρ^{-1} is due to the small difference between the parameter sets for the two properties. A similar agreement can be seen between the theoretical and experimental Φ. The former has been calculated with the aid of the touched-bead theory[16] of $[\eta]$ for $M_w > 5 \times 10^4$; the dashed line connects the theoretical Φ values corresponding to $[\eta]$ for two beads (the left end of the solid curve) and the Einstein sphere limit (*i.e.*, $L = d$). The sudden decrease in experimental Φ for $M_w < 2 \times 10^4$ with decreasing molecular weight cannot be explained by the discrete-chain theory, but the sphere-limiting value does not seem to deviate much from the experimental Φ–M_w relation in the region of $M_w \sim 1.5 \times 10^4$.

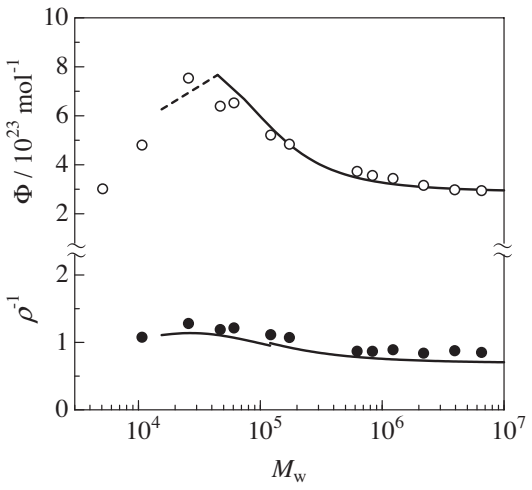

Figure 6. Molecular weight dependence of ρ^{-1} and Φ for polymacromonomer F15 in cyclohexane at 34.5 °C. Solid lines, theoretical values for the wormlike chain model[13–16] with $M_L = 6200\,\mathrm{nm}^{-1}$, $\lambda^{-1} = 9.5\,\mathrm{nm}$, $d = 4.7\,\mathrm{nm}$, and $\delta = 2.2\,\mathrm{nm}$. See the text for the dashed line.

CONCLUSIONS

We may draw the following conclusions from the SAXS data obtained for polystyrene polymacromonomer samples with a side chain length of 15 styrene units in cyclohexane at 34.5 °C. The effects of chain thickness and ends on $\langle S^2\rangle_z$ are significant in the molecular weight region studied, *i.e.*, for $M_w < 2 \times 10^5$, and their consideration allows the present $\langle S^2\rangle_z$ and $P(\theta)$ data and previous light scattering $\langle S^2\rangle_z$ data to be explained consistently by the wormlike cylinder with $M_L = 6200\,\mathrm{nm}^{-1}$, $\lambda^{-1} = 9.5\,\mathrm{nm}$, $d = 4.8 \pm 0.3$ nm, and δ (the end effect parameter) $= 2.2\,\mathrm{nm}$ over a broad range of M_w. This parameter set is essentially the same as that describing the molecular weight dependence of $[\eta]$ and D for the polystyrene polymacromonomer in the theta solvent. Unless the axial ratio is less than 2 (the number of side chains is less than 10), the conventional cross-section plot of $\ln[kP(\theta)]$ *vs.* k^2 with slope $-d^2/16$ gives d values that agree with those evaluated from curve-fitting of the scattering functions. The semiflexible comb model, composed of wormlike main and side chains, also describes the $\langle S^2\rangle_z$–M_w relationship and the angular dependence of $k^2P(\theta)$ for $k < 1\,\mathrm{nm}^{-1}$ if we choose the Kuhn segment length of the side chain to be 6 nm, a value considerably larger than that known for the linear polystyrene molecule (2 nm).

APPENDIX

This appendix presents the expressions for $\langle S^2 \rangle$ and $P(\theta)$ of a semiflexible comb composed of wormlike main and side chains, in relation to the data analyses made in Figures 3 and 5b. The side chains, each having a contour length L_s and a Kuhn length λ_s^{-1}, are connected to the main chain of contour length L and Kuhn length λ^{-1} at intervals of L_c $[= L/(p+1)]$ by universal joints, where p denotes the number of side chains or the number of junction points in the molecule. Thus the total contour length L_t of the semiflexible comb is given by $L_t = pL_s + L$. The expression for $\langle S^2 \rangle$ of this molecule derived by Nakamura *et al.*[26] reads

$$\langle S^2 \rangle = \langle S^2 \rangle_s + \langle S^2 \rangle_m \tag{A-1}$$

where

$$\begin{aligned}\langle S^2 \rangle_s = \frac{p}{{L_t}^2} \Bigg\{ {L_s}^2 \left[\frac{L_s}{6\lambda_s} - \frac{1}{4{\lambda_s}^2} + \frac{1}{4{\lambda_s}^3 L_s} - \frac{1}{8{\lambda_s}^4 {L_s}^2} \left(1 - \mathrm{e}^{-2\lambda_s L_s}\right) \right] \\ + L_s (L_t - L_s) \left[\frac{L_s}{2\lambda_s} - \frac{1}{2{\lambda_s}^2} + \frac{1}{4{\lambda_s}^3 L_s} \left(1 - \mathrm{e}^{-2\lambda_s L_s}\right) \right] \Bigg\}\end{aligned} \tag{A-2}$$

and

$$\begin{aligned}\langle S^2 \rangle_m = \frac{1}{{L_t}^2} \Bigg\{ L^2 \left[\frac{L}{6\lambda} - \frac{1}{4\lambda^2} + \frac{1}{4\lambda^3 L} - \frac{1}{8\lambda^4 L^2} \left(1 - \mathrm{e}^{-2\lambda L}\right) \right] \\ + L_s L \left[\frac{2p+1}{p+1} \frac{pL}{6\lambda} - \frac{p}{2\lambda^2} + \frac{p}{2\lambda^3 L} - \frac{1}{2\lambda^3 L} \frac{\mathrm{e}^{-2\lambda L_c}}{1 - \mathrm{e}^{-2\lambda L_c}} \left(1 - \mathrm{e}^{-2\lambda L_c p}\right) \right] \\ + {L_s}^2 \left[p(p-1) \left(\frac{L}{6\lambda} - \frac{1}{4\lambda^2} \right) + \frac{1}{2\lambda^2} \frac{\mathrm{e}^{-2\lambda L_c}}{1 - \mathrm{e}^{-2\lambda L_c}} \left(p - \frac{1 - \mathrm{e}^{-2\lambda L_c p}}{1 - \mathrm{e}^{-2\lambda L_c}} \right) \right] \Bigg\}\end{aligned} \tag{A-3}$$

The particle scattering function for the same model chain as above may be calculated from

$$P(\theta) = 2(J_1 + J_2 + J_3 + J_4)/{L_t}^2 \tag{A-4}$$

with

$$J_1 = \int_0^L (L - t) I(k; t)\, \mathrm{d}t \tag{A-5}$$

$$J_2 = p \int_0^{L_s} (L_s - t) I(k; t)\, \mathrm{d}t \tag{A-6}$$

$$J_3 = 2 \sum_{i=1}^{p} \int_0^L I(k; s_{i0} - s)\, \mathrm{d}s \int_0^{L_s} I(k; s_i)\, \mathrm{d}s_i \tag{A-7}$$

$$J_4 = \sum_{i=1}^{p-1} \sum_{j=i+1}^{p} I(k; s_{j0} - s_{i0}) \times \int_0^{L_s} I(k; s_i)\, \mathrm{d}s_i \int_0^{L_s} I(k; s_j)\, \mathrm{d}s_j \tag{A-8}$$

and

$$I(k; t) = \langle \exp[\mathrm{i}\mathbf{k} \cdot \mathbf{R}(t)] \rangle \tag{A-9}$$

In these equations, $\mathbf{R}(t)$ is the distance vector between contour points s and s' $(t = |s' - s|)$, s_{x0} $(x = i, j)$ denotes the contour point on the main chain at which the xth side chain is connected, and the contributions J_1, J_2, ..., J_4 correspond to the cases in which (1) two points s and s' are on the main chain, (2) they are on the same side chain, (3) s is on the main chain and s_i is on the ith side chain, and (4) s_i and s_j are on the ith and jth side chains, respectively. For computing J_1, J_2, ..., J_4, we use the interpolation expression of $I(k, t)$ obtained by Nakamura and Norisuye.[20]

The above eqs A-4 through A-9 are concerned with the comb molecule composed of infinitely thin main and side chains. If the thickness is introduced into these sub-chains by use of the touched-bead model with bead diameter d_b,[28] the desired $P(\theta)$ is expressed by

$$\begin{aligned}P(\theta) = 9 \left(\frac{2}{kd_b} \right)^6 [\sin(kd_b/2) \\ - (kd_b/2)\cos(kd_b/2)]^2 P_0(\theta)\end{aligned} \tag{A-10}$$

where $P_0(\theta)$ denotes the scattering function (eq A-4) for the comb consisting of infinitely thin sub-chains.

REFERENCES

1. M. Wintermantel, M. Schmidt, Y. Tsukahara, K. Kajiwara, and S. Kohjiya, *Macromol. Rapid Commun.*, **15**, 279 (1994).
2. N. Nemoto, M. Nagai, A. Koike, and S. Okada, *Macromolecules*, **28**, 3854 (1995).
3. M. Wintermantel, M. Gerle, K. Fischer, M. Schmidt, I. Wataoka, H. Urakawa, K. Kajiwara, and Y. Tsukahara, *Macromolecules*, **29**, 978 (1996).
4. S. Kawaguchi, K. Akaike, Z.-M. Zhang, H. Matsumoto, and K. Ito, *Polym. J.*, **30**, 1004 (1998).
5. K. Fischer and M. Schmidt, *Macromol. Rapid Commun.*, **22**, 787 (2001).

6. S. Lecommandoux, F. Checot, R. Borsali, M. Schappacher, A. Deffieux, A. Brulet, and J. P. Cotton, *Macromolecules*, **35**, 8878 (2002).
7. K. Terao, Y. Takeo, M. Tazaki, Y. Nakamura, and T. Norisuye, *Polym. J.*, **31**, 193 (1999).
8. K. Terao, Y. Nakamura, and T. Norisuye, *Macromolecules*, **32**, 711 (1999).
9. T. Hokajo, K. Terao, Y. Nakamura, and T. Norisuye, *Polym. J.*, **33**, 481 (2001).
10. K. Terao, S. Hayashi, Y. Nakamura, and T. Norisuye, *Polym. Bull.*, **44**, 309 (2000).
11. K. Terao, T. Hokajo, Y. Nakamura, and T. Norisuye, *Macromolecules*, **32**, 3690 (1999).
12. H. Yamakawa, "Helical Wormlike Chains in Polymer Solutions," Springer, Berlin, 1997.
13. H. Benoit and P. Doty, *J. Phys. Chem.*, **57**, 958 (1953).
14. H. Yamakawa and M. Fujii, *Macromolecules*, **6**, 407 (1973).
15. T. Norisuye, M. Motowoka, and H. Fujita, *Macromolecules*, **12**, 320 (1979).
16. T. Yoshizaki, I. Nitta, and H. Yamakawa, *Macromolecules*, **21**, 165 (1988).
17. T. Norisuye, *Prog. Polym. Sci.*, **18**, 543 (1993).
18. O. Glatter and O. Kratky, "Small Angle X-ray Scattering," Academic Press, London, U.K., 1982.
19. I. Wataoka, H. Urakawa, K. Kajiwara, M. Schmidt, and M. Wintermantel, *Polym. Int.*, **44**, 365 (1997).
20. Y. Nakamura and T. Norisuye, *J. Polym. Sci., Part B: Polym. Phys.*, **42**, 1398 (2004).
21. K. Nagasaka, T. Yoshizaki, J. Shimada, and H. Yamakawa, *Macromolecules*, **24**, 924 (1991).
22. Y. Nakamura, K. Amitani, K. Terao, and T. Norisuye, *Kobunshi Ronbunshu*, **60**, 176 (2003).
23. Y. Nakamura, K. Akashi, T. Norisuye, A. Teramoto, and M. Sato, *Polym. Bull.*, **38**, 469 (1997).
24. O. Kratky and G. Porod, *Recl. Trav. Chim. Pays-Bas*, **68**, 1106 (1949).
25. T. Konishi, T. Yoshizaki, T. Saito, Y. Einaga, and H. Yamakawa, *Macromolecules*, **23**, 290 (1990).
26. Y. Nakamura, Y. Wan, J. W. Mays, H. Iatrou, and N. Hadjichristidis, *Macromolecules*, **33**, 8323 (2000).
27. T. Norisuye and H. Fujita, *Polym. J.*, **14**, 143 (1982).
28. W. Burchard and K. Kajiwara, *Proc. R. Soc. London, Ser. A*, **316**, 185 (1970).